PERGAMON

International Journal of Heat and Mass Transfer 44 (2001) 2405–2411

International Journal of HEAT and MASS TRANSFER

www.elsevier.com/locate/ijhmt

# Interactive thermal and solutal Marangoni convection during compound semiconductor growth in a rectangular open boat

K. Arafune *, K. Yamamoto, A. Hirata

*Department of Chemical Engineering, Waseda University 3-4-1 Okubo, Shinjuku-ku, Tokyo 169-8555, Japan*

Received 11 May 2000; received in revised form 6 September 2000

**Abstract**

An experimental study was performed on Marangoni convection due to temperature and concentration gradients on a free surface during InSb crystal growth. InSb was grown from $In_xSb_{1-x}$ melt one directionally in a carbon rectangular crucible. The velocities on the free surface were measured in two cases: one is that the directions of the driving forces for thermal and solutal convection are the same (acceleration case), and the other is that the directions of the driving forces are opposite (deceleration case). In the deceleration case, the flow direction on the free surface is from the crystal–melt interface to the bulk of the melt. This flow direction is opposite to the flow direction without consideration of solutal convection. 

## 1. Introduction

Since the transistor was invented, a semiconductor, especially a silicon crystal, is one of the most important materials that support highly developed information society. Compound semiconductors are also powerful materials for electric and opt-electric devices, because band gaps of compound semiconductors can be changed continuously by changing composition. Although the growth of bulk compound semiconductors has been studied by many investigators, the number of compound semiconductors that could be used for practical purposes is limited. One of the reasons is that most of the grown crystals have not sufficient quality for practical use. To make high-quality bulk single crystals, it is necessary to clarify and to control phenomena that occur in crystal growth processes. Above all, convection strongly affects heat and mass transport phenomena when a crystal is grown from melt. Therefore, many investigators have attempted to clarify the mechanism of convection during crystal growth using the Czochralski (CZ) [1–4], the Floating Zone (FZ) [5–8], and the Horizontal Bridgman (HB) [9–13] methods. These studies were concerned with thermal buoyancy and/or Marangoni convection. For most of the compound semiconductors, the crystal and melt compositions are different when the crystal is grown from melt, and the compositions change with the crystal growing. As density and surface tension of melt are functions of concentration, solutal convection occurs inside the melt. Although solutal convection due to density difference was studied by many investigators as a double diffusion problem, solutal convection due to surface tension difference was reported in several cases [14–18]. A parametric study of solutal Marangoni convection in a cavity was performed numerically by Polezhaev et al. [14]. The authors' group carried out the "Mixing of melt of multicomponent of compound semiconductor" experiment utilizing solutal Marangoni convection in the Second International Microgravity Laboratory (IML-2) aboard the space shuttle in 1994. From the experimental results and numerical simulation, it was found that solutal Marangoni convection is very effective for liquid mixing under microgravity conditions [15,16]. Moreover, we found that typical surface velocity of solutal Marangoni convection is about 3–5 times higher than that of thermal Marangoni convection [17]. These studies demonstrated that solutal Marangoni convection plays an important role in compound semiconductor growth. Therefore, the objective of the present

* Corresponding author. Tel.: +81-3-5286-3213; fax: +81-3-3232-7083.

*E-mail address:* ara@t3.rim.or.jp (K. Arafune).

0017-9310/01/$ - see front matter 
PII: S0017-9310(00)00284-2

**Nomenclature**

| | |
|---|---|
| $D$ | depth of melt [m] |
| $g$ | gravitational acceleration [m/s$^2$] |
| $Gr_S$ | solutal Grashof number, $g\beta_S\Delta x D^3/v^2$ |
| $Gr_T$ | thermal Grashof number, $g\beta_T\Delta T D^3/v^2$ |
| $k$ | segregation coefficient of Sb |
| $L$ | length of crucible [m] |
| $L_C$ | length of crystal [m] |
| $Ma$ | overall Marangoni number, $Ma_S + \delta Ma_T$ |
| $Ma_S$ | solutal Marangoni number, $\lvert\partial\sigma/\partial x\rvert\Delta x (L - L_C)/\mu v$ |
| $Ma_T$ | thermal Marangoni number, $\lvert\partial\sigma/\partial T\rvert\Delta T (L - L_C)/\mu v$ |
| $Pr$ | Prandtl number, $v/\alpha$ |
| $Re$ | Reynolds number, $(u\lvert(L - L_C)/v)$ |
| $T$ | temperature [°C] |
| $u$ | typical surface velocity [m/s] |
| $x$ | composition of Sb |

*Greek symbols*

| | |
|---|---|
| $\alpha$ | thermal diffusivity [m$^2$/s] |
| $\beta_S$ | solutal expansion coefficient |
| $\beta_T$ | thermal expansion coefficient [1/°C] |
| $\delta$ | $\delta = 1$; in acceleration case, $\delta = -1$; in deceleration case |
| $\Delta T$ | temperature difference, $T_H - T_C$ [°C] |
| $\Delta x$ | concentration difference $= \lvert x_{bulk} - x_{melt}\rvert$ |
| $\mu$ | viscosity [kg/m/s] |
| $v$ | kinematic viscosity [m$^2$/s] |
| $\rho$ | density [kg/m$^3$] |
| $\sigma$ | surface tension [N/m] |

*Subscripts*

| | |
|---|---|
| bulk | at bulk of melt |
| C | at cold side of crucible |
| CM | at crystal–melt interface |
| cryst | at crystal side near crystal–melt interface |
| H | at hot side of crucible |
| init | initial value |
| M | at middle of crucible |
| melt | at melt side near crystal–melt interface |
| S | seed crystal |

study is to investigate interaction between thermal and solutal Marangoni convection during compound semiconductor growth. It is an extension of the work by authors [18] in which interactive thermal and solutal Marangoni convection in a rectangular open boat was investigated numerically.

The directions of the driving forces due to temperature difference cannot be changed during crystal growth. Therefore, to investigate interactive thermal and solutal convection, it is important to change the directions of the driving forces due to concentration difference. In order to change the concentration difference significantly without changing component materials, In–Sb system was selected as a test sample. The segregation coefficient of Sb $k$ $(= x_{cryst}/x_{melt})$ is determined by the phase diagram of In–Sb system [19] shown in Fig. 1. Here, $x_{cryst}$ and $x_{melt}$ are the crystal and the melt composition near the crystal–melt (C–M) interface, respectively. When $0 < x_{melt} < 0.5, k$ is more than 1, so that $x_{melt}$ is less than the melt composition at the bulk of the melt $x_{bulk}$. Oppositely, when $0.5 < x_{melt} < 0.68$, $k$ is less than 1, so that $x_{melt}$ is more than $x_{bulk}$. In addition, when $x_{melt}$ equals to 0.5, $k$ equals to 1, so that only thermal convection exists in the melt. In this study, we observed the surface flow in three cases as mentioned above.

## 2. Experimental procedure

Since the generation of Marangoni convection is prevented by the formation of metal oxide film on the free surface, it is necessary to take special care concerning oxidation of the melt. In preparing test sample, $In_{1-x}Sb_x$, In and Sb (5N, manufactured by Dowa Mining) were mixed in designated ratio, and the mixture was melted and quenched in oxygen reducing atmosphere (Ar 97% + $H_2$ 3%). Then chemical etching for the test sample was done. Moreover, a carbon crucible was baked for degassing. Fig. 2 shows a cross-section of the carbon crucible. The test sample was set in the reservoir tank, and InSb, which has a length of approximately 20 mm, was also set at the cold side of the observation part as a seed crystal (Fig. 2(a)). Then, only

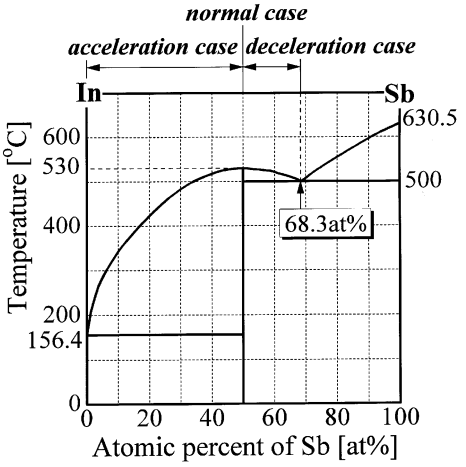


Fig. 1. Phase diagram of In–Sb system [19].

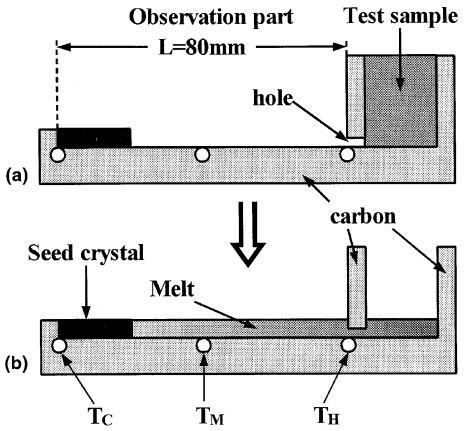


Fig. 2. Cross-section of the carbon crucible; (a) setup, (b) after melting.

the test sample was heated up to its melting point. After melting the test sample, the melt flows into the observation part through a small hole, and it contacts the seed crystal (Fig. 2(b)). Then, the small hole prevents efflux of the remaining metal oxides in the sample.

The experimental system of InSb crystal growth is schematically shown in Fig. 3. The carbon crucible was set in a vacuum chamber, and it was heated from below. The temperatures of the hot side, $T_H$, and the cold side, $T_C$, were controlled by PID temperature controllers with an accuracy better than $\pm 0.1$°C. The temperature difference between $T_H$ and $T_C$ was kept at 40°C, and both temperatures were decreased with the same rate (1°C/min). We measured not only $T_H$ and $T_C$, but also the temperature at the middle of the crucible, $T_M$. To reduce buoyancy convection, we used the shallow crucible. The length ($L$), width, and depth of the crucible are 80, 20, 5 mm, respectively. The test sample was solidified one directionally in the crucible similar to the HB method. To measure the velocity on the free surface, boron nitride (BN) particles were used as tracers. The

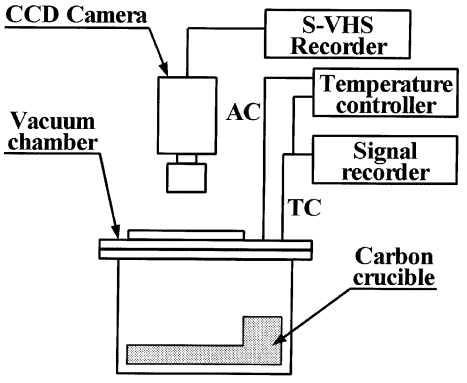


Fig. 3. Schematic diagram of the experimental system.

surface flow can be observed by means of a 3-CCD video camera, and it was recorded by means of a super-VHS recorder with frame rate of 60 1/s. The surface velocity measurement was performed by tracing the BN particles.

We prepared the test samples for $x_{init} = 0.45, 0.5$, 0.55, and 0.6. Here, $x_{init}$ is the initial composition of the test sample. For In–Sb system, $\partial\rho/\partial T, \partial\rho/\partial x, \partial\sigma/\partial T$, and $\partial\sigma/\partial x$ are negative. Here, $\rho$ and $\sigma$ are density and surface tension of the melt. Taking these features of physical properties of the melt and the In–Sb phase diagram into consideration, experimental conditions are arranged as follows.

(a) *Acceleration case* ($0 < x_{init} < 0.5$): The directions of the driving forces due to the concentration difference and the temperature difference are the same.

(b) *Normal case* ($x_{init} = 0.5$): Only the driving force due to the temperature difference exists.

(c) *Deceleration case* ($0.5 < x_{init} < 0.68$): The directions of the driving forces are opposite.

Schematic drawing of the directions of the driving forces is shown in Fig. 4.

To evaluate the effect of buoyancy force on the surface velocity, we carried out the experiments for $x_{init} = 0.6$ during parabolic flights by using MU-300 airplane. In the airplane, gravity fields can be varied from 0.01 to $2g$ by the engine power and the posture of the airplane. When the gravity level equals to $0.01g$, in order to reduce G-jitter, the vacuum chamber and the CCD camera were installed in the payload of the Large Scale Active Vibration Isolation System (developed by Ishikawajima-Harima Heavy Industries).

## 3. Results and discussion

If the crystal growth rate was changed with time, the effect of the crystal growth rate on the flow had to be

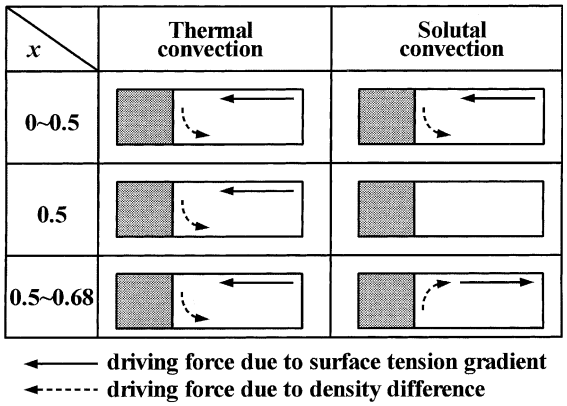


Fig. 4. Schematic drawing of the directions of the driving forces.

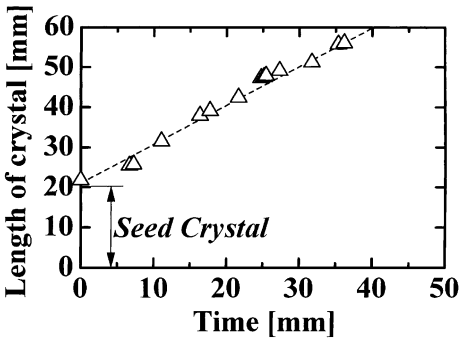


Fig. 5. Time course of the crystal length for $x_{init} = 0.45$.

considered. Therefore, keeping the constant growth rate is favorable. Fig. 5 shows the time course of the crystal length, $L_C$, for $x_{init} = 0.45$. The growth rate for $x_{init} = 0.45$ is almost constant, and similar results are obtained for other $x_{init}$. However, the values of the growth rates are slightly different from each other. To compare with the change of the surface flow in all cases, we use the crystal length instead of the time.

Fig. 6 shows the relationship between $L_C$ and the typical free surface velocity that was measured at about 10 mm from the C–M interface. When $x_{init}$ equals to 0.5 (Fig. 6(a)), $k$ equals to 1, so that it is considered that only the thermal convection exists in the melt (normal case). In this case, the direction of the surface flow is from the bulk of the melt to the C–M interface. When $x_{init}$ equals to 0.45 (Fig. 6(b)), $k$ is more than 1, so that, it is considered that the surface flow directions of thermal and solutal convection are the same, and both convections accelerate each other (acceleration case). Comparing Fig. 6(b) with Fig. 6(a), the typical surface velocities in the acceleration case are much higher than those in the normal case. When $x_{init}$ equals to 0.55 and 0.6 (Fig. 6(c) and (d)), $k$ is less than 1. In these cases, it is considered that the surface flow directions of thermal and solutal convection are opposite (deceleration case). The surface flow direction in the deceleration case is from the C–M interface to the bulk of the melt, and it is opposite to the direction in the normal and the acceleration cases. This result suggests clearly that the solutal convection dominates the direction of the surface flow near the C–M interface. However, it is not clear which of solutal Marangoni and buoyancy convection dominates the flow direction. To evaluate the driving force of solutal Marangoni and buoyancy convection, we estimated $x_{bulk}$ and $x_{melt}$ as a driving force of the solutal convection.

Since the growth crystals were InSb in all cases, $x_{bulk}$ was estimated by the following equation:

$$x_{bulk} = \frac{x_S L_S + x_{init}(L - L_S) - \int_0^{L_C} x_{cryst}\, d\ell}{L - L_C}. \quad (1)$$

Here, $x_S$ and $L_S$ are the composition and the length of the seed crystal, respectively. In this study, growth crystals are InSb in all cases, so that $x_{cryst}$ equals to 0.5.

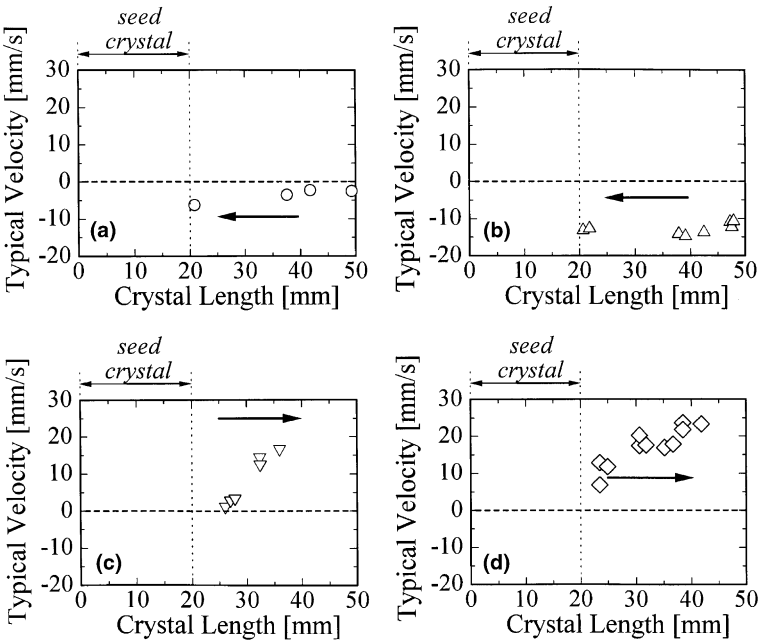


Fig. 6. Relationship between the crystal length and the typical surface velocity at about 10 mm from the C–M interface, arrows show the direction of the flow near the C–M interface: (a) $x_{init} = 0.5$; (b) $x_{init} = 0.45$; (c) $x_{init} = 0.55$; (d) $x_{init} = 0.6$.

$x_{melt}$ was estimated by means of the temperature at the C–M interface $T_{CM}$ and the phase diagram of In–Sb system shown in Fig. 1. Although the thermal conductivity of InSb melt was reported by many researchers, the values were different from each other [20,21]. In addition, the thermal conductivity of In–Sb mixture has not been reported. Therefore, in order to estimate $T_{CM}$ without using the thermal conductivity, we assumed that temperature gradients at the grown crystal, $(dT/d\ell)|_{cryst}$, and the melt, $(dT/d\ell)|_{melt}$, are constant, and calculated $T_{CM}$ by using the following equations:

$$T_{CM} = T_H - \frac{(T_H - T_M) \times (L - L_C)}{L/2} \quad \text{for } L_C \leqslant L/2, \tag{2}$$

$$T_{CM} = T_C + \frac{(T_M - T_C) \times L_C}{L/2} \quad \text{for } L_C > L/2. \tag{3}$$

Fig. 7 shows the relationship between $L_C$ and the estimated Sb compositions. In order to judge which of the thermal and the solutal buoyancy effects is dominant, we calculated solutal Grashof number $Gr_S$, and thermal Grashof number $Gr_T$. Here, the depth of the melt $D$ was used as the characteristic length of Grashof number, because the buoyancy force works in the direction of the gravity force. In all cases, $Gr_S/Gr_T$ ranges between 0.3 and 0.6. It means that the magnitude of the solutal buoyancy effect is smaller than that of the thermal buoyancy effect. In the same way, we calculated solutal Marangoni number $Ma_S$, thermal Marangoni number $Ma_T$. Here, the length of the free surface, $L - L_C$, was used as the characteristic length of Marangoni number, because the Marangoni effect appears at the free surface. In all cases $Ma_S/Ma_T$ ranges between 1.7 and 3.8. It means that the magnitude of the solutal Marangoni effect is larger than that of the thermal Marangoni effect. As mentioned before, the solutal convection dominates the direction of the surface flow near the C–M interface. Therefore, it is obvious that the solutal Marangoni effect is the most important for the surface flow near the C–M interface.

In order to make sure that the Marangoni convection is dominant in the melt, we carried out the experiments for $x_{init} = 0.6$ during parabolic flights. Since the gravity level could be varied from 0.01 to 2$g$, we could observe the effect of buoyancy convection on the free surface velocity without changing the effect of Marangoni convection on it. Fig. 8 shows the effect of gravity level on the free surface velocity near the C–M interface when $x_{init}$ and $L_C$ equal to 0.6 and about 35 mm, respectively. If the buoyancy effect dominates the surface flow near the C–M interface, the surface velocity must decrease with decreasing gravity level. However, the surface velocity is kept constant at about 20 mm/s when the gravity level is below 1.4$g$. On the other hand, when the gravity level exceeds 1.4$g$, the surface velocity increases with increasing gravity level. This result also indicates

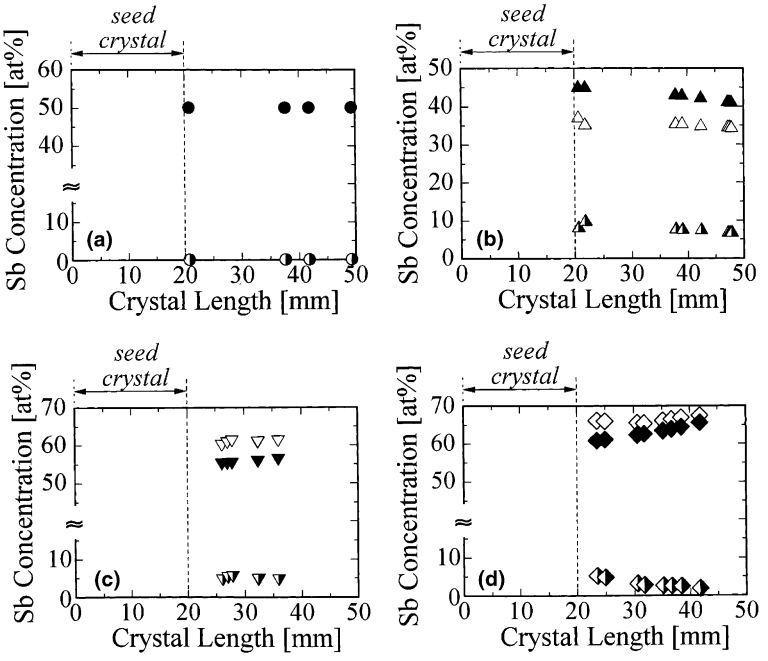


Fig. 7. Relationship between the crystal length and the estimated Sb concentration: (a) $x_{init} = 0.5$; (b) $x_{init} = 0.45$; (c) $x_{init} = 0.55$; (d) $x_{init} = 0.6$; open symbols: concentration at the C–M interface, closed symbols: bulk concentration, half closed symbols: concentration difference.

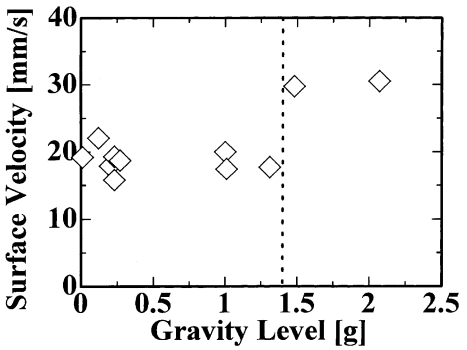


Fig. 8. Effect of the gravity level on the free surface velocity; $x_{init} = 0.6$, $L_C \approx 35$ mm.

that the surface velocity near the C–M interface is dependent on solutal Marangoni convection under the normal gravity condition.

In our recent work [17], we clarified that the solutal Marangoni convection can be treated as similar way as the thermal Marangoni convection using dimensionless parameter, *Ma*, *Pr*, and *Re*. Fig. 9 shows the relationship between $MaPr^{-1/2}$ and *Re*. It seems that *Re* is proportional to $MaPr^{-1/2}$ to the power of 2/3, except for $x_{init} = 0.45$ (acceleration case). There are two reasons for the difference between the result of $x_{init} = 0.45$ and the other results. One is that the free surface is contaminated by metal oxides when $x_{init}$ equals to 0.45. However, this reason is not suitable on the grounds that the surface velocities except for $x_{init} = 0.45$ were not reduced. The other reason is that the solutal Marangoni convection does not affect the surface velocity in the acceleration

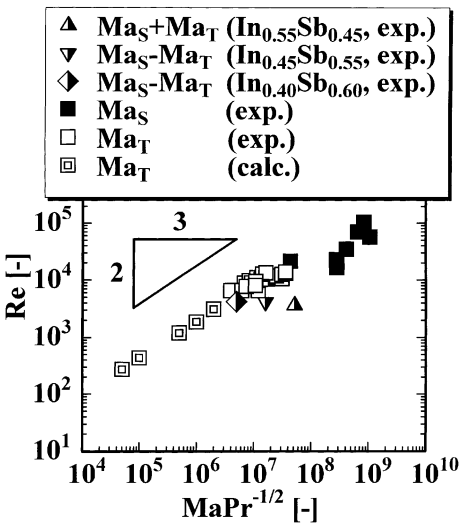


Fig. 9. Relationship between $MaPr^{-1/2}$ and *Re*; square plots are results of solutal or thermal Marangoni convection, half closed symbols are results of solutal and thermal Marangoni convection.

case. In the acceleration case, the direction of the surface flow is from the bulk of the melt to the C–M interface. Since the surface flow suppresses the mass transport from the C–M interface, concentration gradient is difficult to be formed along the free surface. If we do not take the solutal Marangoni effect into consideration, $MaPr^{-1/2}$ is about $1 \times 10^7$. In this case, the result of $x_{init} = 0.45$ agrees with the other results. Consequently, the solutal Marangoni effect is negligible in the acceleration case, and the interactive thermal and solutal Marangoni convection in the deceleration case can be described as similar way as the thermal Marangoni convection by using the difference between the solutal and thermal Marangoni effects.

## 4. Conclusion

Interactive thermal and solutal convection during InSb crystal growth from $In_{1-x}Sb_x$ melt was experimentally studied in the present work. As a result, we found the following three cases:

(a) *Acceleration case*: The directions of the driving forces due to the concentration difference and the temperature difference are the same.

(b) *Normal case*: Only the driving force due to the temperature difference exists.

(c) *Deceleration case*: The directions of the driving forces are opposite.

Especially in the deceleration case, it was observed that the direction of the surface flow was from the C–M interface to the bulk of the melt. This flow direction is opposite to the flow direction without consideration of solutal convection. From the evaluation using dimensionless numbers and the parabolic flight experiments, it is clear that the solutal Marangoni effect is dominant in the melt flow near the C–M interface. Moreover, it was shown that the solutal Marangoni effect is negligible in the acceleration case, and the interactive thermal and solutal Marangoni convection in the deceleration case can be described as same as the thermal Marangoni convection by using the difference between the solutal and thermal Marangoni effects. Although the solutal convection had been neglected, this study demonstrated that the solutal convection, particularly solutal Marangoni convection, plays an important part in compound semiconductor growth with free surface.

## Acknowledgements

The authors wish to thank Mr. M. Sugiura for assistance with the experiments. A part of this work was supported by a Grant-in-Aid for General Scientific Research (B) (No. 11694176) from Japan Society for the Promotion of Science.

## References


[1] R. Lamprecht, D. Schwabe, A. Scharmann, E. Schultheiss, Experiments on buoyant, thermocapillary, and forced convection in Czochralski configuration, J. Cryst. Growth 65 (1983) 143–152.

[2] K. Kakimoto, M. Watanabe, M. Eguchi, T. Hibiya, Ordered structure in non-axisymmetric flow of silicon melt convection, J. Cryst. Growth 126 (1993) 435–440.

[3] A. Hirata, M. Tachibana, T. Sugimoto, Y. Okano, T. Fukuda, Control of crystal–melt interface shape during growth of lithium niobate single crystal, J. Cryst. Growth 131 (1993) 145–152.

[4] T. Tsukada, K. Kakinoki, M. Hozawa, N. Imaishi, Effect of internal radiation within crystal and melt on Czochralski crystal growth of oxide, Int. J. Heat Mass Transfer 38 (1995) 2707–2714.

[5] Ch.-H. Chun, Marangoni convection in a floating zone under reduced gravity, J. Cryst. Growth 48 (1980) 600–610.

[6] Y. Okano, A. Hatano, A. Hirata, Natural and Marangoni convections in a floating zone, J. Chem. Eng. Jpn. 22 (1989) 385–388.

[7] C.W. Lan, Heat transfer, fluid flow, and interface shapes in the floating-zone growth of tube crystals, J. Cryst. Growth 141 (1994) 265–278.

[8] Q.S. Chen, W.R. Hu, Numerical investigation on a simulation model of floating zone convection, Int. J. Heat Mass Transfer 40 (1997) 757–763.

[9] D.T.J. Hurle, Temperature oscillations in molten metals and their relationship to growth striae in melt-grown crystals, Philos. Mag. 13 (1966) 305–310.

[10] Y. Okano, M. Itoh, A. Hirata, Natural and Marangoni convections in a two-dimensional rectangular open boat, J. Chem. Eng. Jpn. 22 (1989) 275–281.

[11] M. Mundrane, A. Zebib, Two- and three-dimensional buoyant thermocapillary convection, Phys. Fluids A 5 (1993) 810–818.

[12] V. Saß, H.C. Kuhlmann, H.J. Rath, Investigation of three-dimensional thermocapillary convection in a cubic container by a multi-grid method, Int. J. Heat Mass Transfer 39 (1996) 603–613.

[13] K. Arafune, M. Sugiura, A. Hirata, Investigation of thermal Marangoni convection in low- and high-Prandtl number fluids, J. Chem. Eng. Jpn. 32 (1999) 104–109.

[14] V.I. Polezhaev, M.K. Ermakov, Thermosolutal Marangoni convection short-time regimes – proposals for drop tower experiments and real time computer simulation, Microgravity Sci. Technol. V (1992) 172–175.

[15] S. Yasuhiro, T. Sato, N. Imaishi, A. Hirata, M. Kumagawa, Numerical simulation of solutal Marangoni convection during liquid mixing under microgravity, Microgravity Sci. Technol. 9 (1996) 237–244.

[16] K. Okitsu, Y. Hayakawa, A. Hirata, S. Fujiwara, Y. Okano, N. Imaishi, S. Yoda, T. Oida, T. Yamaguchi, M. Kumagawa, Gravitational effects on mixing and growth morphology of an $In_{0.5}Ga_{0.5}Sb$ system, Cryst. Res. Technol. 31 (1996) 969–978.

[17] K. Arafune, A. Hirata, Thermal and solutal Marangoni convection in In–Ga–Sb system, J. Cryst. Growth 197 (1999) 811–817.

[18] K. Arafune, A. Hirata, Interactive solutal and thermal Marangoni convection in a rectangular open boat, Numer. Heat Transfer A 34 (1998) 421–429.

[19] M. Hansen, Constitution of Binary Alloys, 2nd ed., McGraw-Hill, New York, 1986, p. 859.

[20] R.G. Seidensticker, M. Rubenstein, Thermal conductivity of liquid InSb and Ga, J. Appl. Phys. 43 (1972) 584–586.

[21] S. Nakamura, T. Hibiya, F. Yamamoto, Thermal conductivity of GaSb and InSb in solid and liquid states, J. Appl. Phys. 68 (1990) 5125–5127.